

Probing Dynamics of Dark Energy with Supernova, Galaxy Clustering and the Three-Year Wilkinson Microwave Anisotropy Probe (WMAP) Observations

Gong-Bo Zhao¹, Jun-Qing Xia¹, Bo Feng², and Xinmin Zhang¹

¹*Institute of High Energy Physics, Chinese Academy of Science,*

P.O. Box 918-4, Beijing 100049, P. R. China and

²*Research Center for the Early Universe(RESCEU),*

Graduate School of Science, The University of Tokyo, Tokyo 113-0033, Japan

(Dated: September 25, 2018.)

Using the Markov chain Monte Carlo (MCMC) method we perform a global analysis constraining the dynamics of dark energy in light of the supernova (Riess "Gold" samples), galaxy clustering (SDSS 3D power spectra and SDSS Lyman- α forest information) and the latest three-year Wilkinson Microwave Anisotropy Probe (WMAP) observations. We have allowed the dark energy equation of state to get across -1 and pay particular attention to the effects when incorrectly neglecting dark energy perturbations. We find the parameter space of dynamical dark energy is now well constrained and neglecting dark energy perturbations will make the parameter space significantly smaller. Dynamical dark energy model where the equation of state crosses -1 is mildly favored and the standard Λ CDM model is still a good fit to the current data.

Introduction. The recent released three year Wilkinson Microwave Anisotropy Probe observations (WMAP-3)[1, 2] have made so far the most precise probe of the CMB observations. The temperature-temperature correlation power is now cosmic variance limited up to $l \sim 400$ where the glitches on the first peak have now disappeared and the third peak is now detected, which gives rise to a better determination on the matter component of the universe[2]. In particular, the direct detection of the CMB EE polarization spectrum and better measurements of TE spectrum have helped a lot in the determination on the reionization depth, which is now lower than the first year WMAP predictions and with much smaller error bars. This has in turn helped to break the degeneracy between the slope of the primordial scalar spectrum and the reionization depth[1, 2]. Intriguingly now for the fittings to the power law Λ CDM model a Harrison-Zel'dovich spectrum is now excluded to $\sim 3\sigma$ by WMAP alone, which will have profound implications in inflation if further confirmed with higher significance level[1]. In the fittings to a constant equation of state of dark energy, combinations of WMAP with other cosmological constant are consistent with a cosmological constant except for the *WMAP + SDSS* combination, where $w < -1$ is favored a bit more than 1σ [1]. The measurements of the SDSS power spectrum[3] is in some sense currently the most precise probe of the linear galaxy matter power spectrum and will hopefully get significantly improved within the coming few years. If the preference of $w > -1$ holds with the accumulation on dark energy this will also help significantly on our understandings towards dark energy. A cosmological constant, which is theoretically problematic at present[4, 5], will not be the source driving the current accelerated expansion and a favored candidate would be something like quintessence[6, 7]. On the other hand, the observations from the Type Ia Supernova (SNIa) in some sense make the only direct detection of dark energy[8, 9, 10, 11, 12] and currently a combination of *WMAP + SNIa* or *CMB + SNIa + LSS*

are well consistent with the cosmological constant and the preference of a quintessence-like equation state has disappeared[1]. Intriguingly, we are also aware that the predictions for the luminosity distance-redshift relationship from the Λ CDM model by WMAP only are in notable discrepancies with the "Gold" samples reported by Riess *et al*[11]. Although the prediction by WMAP is consistent with the measurements from the Supernova Legacy Survey (SNLS)[13], we are aware that the 71 high redshift type Ia supernova alone are too weak for a cosmological probe and even when combined with the 44 nearby SNIa their constraints on dark energy are not yet comparable with the Riess "Gold" sample[13, 14]. Although the discrepancy might be some systematical uncertainties in the Riess "Gold" sample, this needs to be confronted with the accumulation of the 5-year SNLS observations and the ongoing SNIa projects like the Supernova Cosmology Project (SCP) and from the Supernova Search Team (SST). Alternatively, this might be due to the implications of dynamical dark energy.

The rolling scalar field of quintessence typically predicts some evolutions of dark energy equation of state and with the accumulation of the various kinds of observations we are now also able to constrain the dynamics of dark energy over a constant equation of state. Also the WMAP team has considered the constraints on the parameter space where the equation of state is less than -1 . Such an equation of state is originally motivated by the scalar field model of phantom[15], where there is a negative kinetic term and typically w is not a constant either for the case of phantom and it is natural that we can expect a nonzero dw/dz with phantom. The model of phantom has been proposed in history due to the mild preference for a constant $w < -1$ by the observations[15]. Although phantom violates the weak energy condition(WEC) and faces the dilemma of quantum instabilities[16], it remains possible in the description of the nature of dark energy[17].

Previously with the accumulation of SNIa data

and especially after the SNIa observations from the HST/GOODS program[11], many groups have started to probe the time dependence of dark energy equation of state [18, 19, 20, 21, 22]. Intriguingly an equation of state which crosses the cosmological constant boundary are somewhat favored[18, 19, 20, 21]. Such a kind of behavior is nontrivial physically since conventional quintessence and phantom cannot realize such a behavior. In Ref.[21] we dubbed the new kind of dark energy *quintom* in the sense that it resembles the combined behavior of quintessence and phantom. Although the model of k-essence which has non-canonical kinetic term[23, 24] can both have a quintessence and phantom-like behavior, as shown in Refs.[25, 26, 27] a crossing behavior is not viable. Mathematically, the crossing reads that there exists at least one pivot redshift, namely z_i^* satisfies:

$$\frac{dw}{dz} \Big|_{(z_i^*)} \neq 0, w(z_i^*) = -1 \quad (1)$$

where z denotes the redshift and $w(z)$ is the functional form of EOS evolution. Interestingly, the quintom models differ from the quintessence or phantom in evolution and the determination of the fate of universe[28]. There exist lots of interests in the literature presently in building of quintom-like models. For example, with minimally coupled to gravity a simple realization of quintom scenario is a model with the double fields of quintessence and phantom[21, 29, 30, 31, 32, 33, 34, 35, 36]. In such cases quintom would typically encounter the problem of quantum instability inherited from the phantom component. However in the case of the single scalar field model of quintom, Ref.[36] considered a Lagrangian with a high derivative term adding to the kinetic energy and its energy-momentum tensor is equivalent to the two-field quintom model. Such a model is theoretically possible to resolve the problem of quantum instabilities and needs further investigations[37].

Given the lack of theoretical understandings, the cosmological observations play a crucial role to study dark energy. Probing the dynamics of dark energy is of great significance to shed light on theory. SNIa observations which measure the luminosity distance depending on Hubble parameter $H(z)$, are relatively sensitive to the dynamics of dark energy. Moreover, dark energy also leaves imprints on Cosmic Microwave Background(CMB) through the distance to the last scattering surface especially when we take the perturbation of dark energy into consideration. The fluctuations of dark energy can lessen the ISW effect and lowers the power spectrum at small multipoles. Besides affecting $H(a)$, dark energy also modifies the growth rate of structures via perturbation equations. Thus the LSS data such as SDSS 3D power spectrum and Lyman- α forest, can further be used in the determination of the dark energy parameter as well as breaking the degeneracy among the various cosmological parameters.

Given the fact that due to the problems on dark energy perturbations[26] in the conventional parametriza-

tions of dark energy equation of state one cannot make global fittings with w getting across the cosmological constant boundary. Previously for example Ref. [38] studied the perturbations of dynamical dark energy only for the regime where $w > -1$ and Ref. [39] considered both the cases for $w > -1$ and $w < -1$, but did not include the perturbations for quintom like dark energy; while other global analysis like Ref. [40, 41] did not consider dark energy perturbations. In Ref.[26] we gave a method which for the first time allows to study quintom-like dark energy perturbations with parametrization of w , which resembles the behavior of the simplest double-field quintom¹. Our method has allowed a global analysis on the dynamical dark energy equation of state with the observations and like the case for a constant equation of state[42, 43], which has also been recently shown by Spergel *et al*[1], we find incorrectly neglecting dark energy perturbations typically make the parameter space smaller and hence with notable bias.

The aim of current paper is to study the current up-to-date observational constraints on dynamical dark energy. We extend our previous work of Ref.[26] and study the full observational constraints on dynamical dark energy. In particular we pay great attention to the effects of dark energy perturbations when EOS crosses -1 as in (1). Perturbations of the quintom-like models have been studied extensively in Ref.[26]. Our paper is structured as follows: in Section II we describe the method and the data; in Section III we present our results on the determination of cosmological parameters with (WMAP-3) [1, 2], SNIa [11, 13], Sloan Digital Sky Survey 3D power spectrum (SDSS-gal) [3] and SDSS Lyman- α forrest data (SDSS-lya)[44] by global fittings using the Markov chain Monte Carlo (MCMC) techniques [45, 46, 47]; conclusions and discussions in are presented in the last section.

Method and data. In this section we firstly present the general formulae of the dark energy perturbations in the full parameter space of $w(z)$ especially for the crossing models¹. In the global fitting to CMB,SN Ia and LSS data, we adopt the parametrization of EOS as follows:[48]

$$w(z) = w_0 + w_1 \frac{z}{1+z} \quad (2)$$

Despite our ignorance of the nature of dark energy, it is more natural to consider the DE fluctuation whether DE is regarded as scalar field or fluid rather than simply switching it off. The conservation law of energy reads:

$$T_{;\mu}^{\mu\nu} = 0 \quad (3)$$

¹ Although the multi-field dark energy models are more challenging on theoretical aspects of naturalness, given that we know very little on the nature of dark energy, the energy momentum of such models can be identified with single field scalar dark energy with high derivative kinetic terms[36]. Our phenomenological formula of perturbations on DE corresponds to such models of multi-field (quintom) with a negligible difference around the crossing point of -1[26].

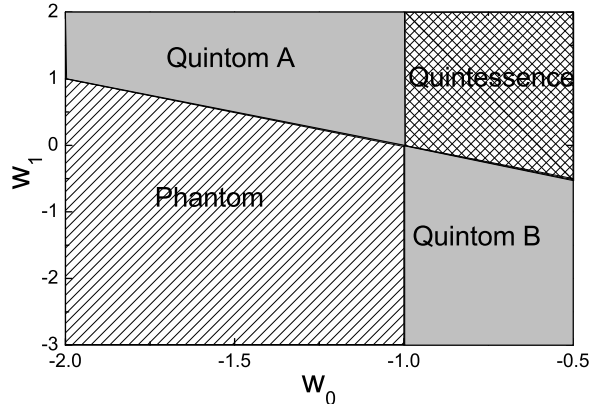


FIG. 1: The lines $w_0 = -1$ and $w_0 + w_1 = -1$ divide the $w_0 - w_1$ parameter space into four parts. The gray-shaded regions are for crossing models where the EOS of "Quintom A" models is greater than -1 in the past and smaller than -1 today while the "Quintom B" models cross -1 in the opposite direction.

where $T^{\mu\nu}$ is the energy-momentum tensor of dark energy and ";" denotes the covariant differentiation. Working in the conformal Newtonian gauge, Equation(3) leads to the perturbation equations of dark energy as follows [49]:

$$\dot{\delta} = -(1+w)(\theta - 3\dot{\Phi}) - 3\mathcal{H}(\delta p/\delta\rho - w)\delta, \quad (4)$$

$$\dot{\theta} = -\mathcal{H}(1-3w)\theta - \frac{\dot{w}}{1+w}\theta + k^2\left(\frac{\delta p/\delta\rho}{1+w}\delta + \Psi\right), \quad (5)$$

$$\delta p = c_s^2\delta\rho + \Gamma\delta S. \quad (6)$$

where c_s^2 is the adiabatic sound speed and $\Gamma\delta S$ is the entropy perturbations. For simplicity we neglect the entropy perturbations and assume the sound speed to be $c_s^2 = 1$ [26]. For the models where the EOS doesn't cross -1, the lower left and the upper right region of FIG.1, the above equation(4), (5) is well defined. For the crossing models in Eq.(1), graphically the gray-shaded area of FIG.1, the perturbation equation (4), (5) is seemingly divergent. However basing on the realistic two-field-quintom model as well as the single field case with a high derivative term [26], the perturbation of DE is shown to be continuous when the EOS gets across -1, thus we introduce a small positive parameter ξ to divide the full range of the allowed value of the EOS w into three parts: 1) $w > -1 + \xi$; 2) $-1 + \xi \geq w \geq -1 - \xi$; and 3) $w < -1 - \xi$.

For the regions 1) and 3) the perturbation is well defined by solving Eqs.(4), (5) as shown above. For the case 2), the perturbation of energy density δ and divergence of velocity, θ , and the time derivatives of δ and θ are finite and continuous for the realistic quintom dark energy models. However for the perturbations with the

above parametrizations clearly there exists some divergence. To eliminate the divergence typically one needs to base on the multi-component DE models which result in the non-practical parameter-doubling. A simple way out is to match the perturbation in region 2) to the regions 1) and 3) at the boundary and set[14, 26, 50]

$$\dot{\delta} = 0, \quad \dot{\theta} = 0. \quad (7)$$

We have numerically checked the error in the range $|\Delta w = \xi| < 10^{-5}$ and found it less than 0.001% to the exact multi-field quintom model. Therefore our matching strategy is a perfect approximation to calculate the perturbation consistently for crossing models(1). For more details of this method we refer the readers to our previous companion papers [14, 26, 50].

We have modified the publicly available Markov Chain Monte Carlo package `camb/cosmomc`[51]² to allow for the inclusion of dark energy perturbations with EOS getting across -1[26] and then sampled from the following 8 dimensional cosmological parameter space using the Metropolis algorithm :

$$\mathbf{p} \equiv (\omega_b, \omega_c, \Theta_S, \tau, w_0, w_1, n_s, \log[10^{10}A_s]) \quad (8)$$

where $\omega_b = \Omega_b h^2$ and $\omega_c = \Omega_c h^2$ are the physical baryon and cold dark matter densities relative to critical density, Θ_S is the ratio (multiplied by 100) of the sound horizon and angular diameter distance, τ is the optical depth, A_s is defined as the amplitude of the primordial scalar power spectrum and n_s measures the spectral index. We have also marginalized over the bias factors b defined as $b = [P_{galaxy}(k)/P(k)]^{1/2}$ which are assumed to be constant. Basing on the Bayesian analysis, we vary the above parameters fitting to the observational data with the MCMC method. Throughout we assume a flat universe and take the weak priors as: $\tau < 0.8, 0.5 < n_s < 1.5, -3 < w_0 < 3, -5 < w_1 < 5, 0.5 < \Theta_S < 10$, a cosmic age tophat prior as $10 \text{ Gyr} < t_0 < 20 \text{ Gyr}$. In addition, we make use of the Hubble Space Telescope (HST) measurement of the Hubble parameter $H_0 = 100h \text{ km s}^{-1} \text{ Mpc}^{-1}$ [52] by multiplying the likelihood by a Gaussian likelihood function peaked at around $h = 0.72$ with a standard deviation $\sigma = 0.08$. We impose a Gaussian prior on the baryon and density $\Omega_b h^2 = 0.022 \pm 0.002$ (1σ) from Big Bang nucleosynthesis[53].

In our calculations we have taken the total likelihood to be the products of the separate likelihoods of CMB, SNIa and LSS. Alternatively defining $\chi^2 = -2 \log \mathcal{L}$, we get

$$\chi_{total}^2 = \chi_{CMB}^2 + \chi_{SNIa}^2 + \chi_{LSS}^2. \quad (9)$$

In the computation of CMB we have included the three-year temperature and polarization data with the routine

² <http://cosmologist.info/cosmomc>
<http://camb.info>

for computing the likelihood supplied by the WMAP team [1, 2]. In the calculation of the likelihood from SNIa, we use the 157 "gold" set of SNIa published by Riess *et al* in Ref.[11] and marginalize over the nuisance parameter. For LSS, we firstly use the code of CAMB to generate the theoretical 3D matter power spectra of every model and fit to SDSS 3D power spectra data[3] using the likelihood code developed in Ref. [54]. To compute the Lyman- α forest likelihood, we use the SDSS Lyman- α data and corresponding likelihood code[44].

Results. In this section we present our results and focus mainly on the dark energy parameters. In particular to show the effects of dark energy perturbations we present the resulting constraints on the parameters for two cases simultaneously: one with and the other (incorrectly) without dark energy perturbations.

In Table 1 we list the mean and 1, 2 σ constraints on dark energy, inflation and reionization related parameters with/without DE perturbations. In our notations in the error bars of the 2 σ constraints we have included the 1 σ contributions of uncertainties. By virtue of the combined data and especially for the new precision WMAP-3 data, we find that all these parameters are well determined in our both cases. The center value of dark energy parameters illustrate the favored dynamical DE models with EOS crossing -1. In our framework of dynamical DE, a lower optical depth τ is still favored which is consistent with the new results of WMAP team[1, 2]. Moreover, a simple scale-invariant primordial spectrum is disfavored at slightly larger than 2- σ even in the presence of dynamical dark energy where the perturbations are included. In fact from Fig.2 we find τ is still well constrained in the present case, which breaks the $n_s - \tau$ degeneracy and favors nontrivially a red primordial scalar spectrum.

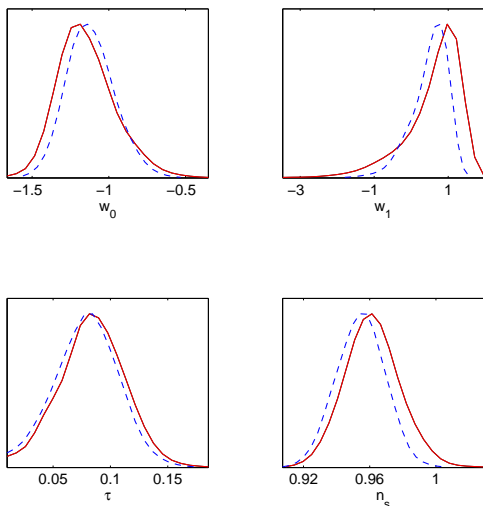


FIG. 2: 1-D constraints on individual parameters using WMAP-3+157 "gold" SNIa+SDSS-gal+SDSS-lya with the model of dynamical dark energy discussed in the text. Red Solid(Blue dashed) curves illustrate the marginalized distribution of each parameter with/without DE perturbation.

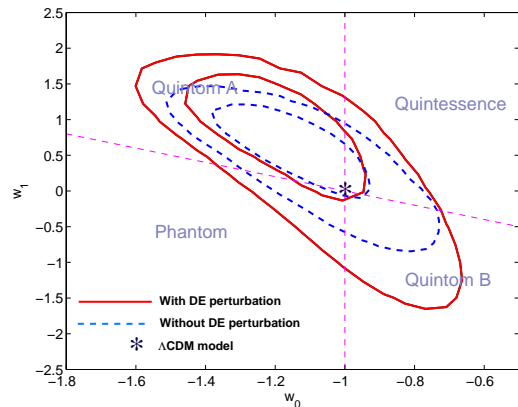


FIG. 3: 68% and 95% constraints of the 2-D contours among dark energy and the background parameters. Red solid and blue dashed lines are for the perturbed and (incorrectly) unperturbed DE respectively.

In Fig.2 we delineate the corresponding posterior one dimensional marginalized distributions of w_0 , w_1 , n_s and τ from our MCMC results. Since the parameters, especially for w_1 , are not perfectly Gaussian distributed, the mean and the marginalized results for each parameter may be different. For the complement of table (1), we find the best fit values constrained by the full dataset is $w_0 = -1.363$, $w_1 = 1.325$, $n_s = 0.964$, $\tau = 0.082$ with DE perturbation and $w_0 = -1.212$, $w_1 = 0.839$, $n_s = 0.953$, $\tau = 0.064$ with when dark energy perturbations are (incorrectly) switched off. One can find that almost all of the best fit parameters have been modified by the effect of DE perturbations. Moreover, the allowed parameter space has been changed a lot and the constraints on the background parameters have been less stringent when including the dark energy perturbations. This can also be clearly seen from the two dimensional contour plots in Fig.3. The reason is not difficult to explain. The ISW effects of the dynamical dark energy boosts the large scale power spectrum of CMB[26]. For a constant equation of state Ref. [42] has shown that when the perturbations of dark energy have been neglected incorrectly, a suppressed ISW will be resulted for quintessence-like dark energy and on the contrary, an enhanced ISW is led to by phantom-like dark energy. In this sense if we neglect dark energy contributions, there will be less degeneracy in the determination of dark energy as well as the relative cosmological parameters. However, dark energy perturbations are anti-correlated with the source of matter perturbations and this will lead to a compensation on the ISW effects, which result in a large parameter degeneracy[42]. In fact as we have shown that crossing over the cosmological constant boundary would not lead to distinctive effects[26], hence the effects of our smooth parametrization of EOS on CMB can also be somewhat

TABLE 1. Mean and $1, 2\sigma$ constrains on dark energy, spectral index and optical depth parameters using the combined data of WMAP-3, "Gold" SNIa sample, SDSS 3D power spectra and SDSS lyman- α forest information with/without DE perturbation. Note that in the error bars of the 2σ constraints we have included the 1σ contributions of uncertainties.

parameter	WMAP-3+RIESS + SDSS-gal + SDSS-lya	
	With Dark Energy perturbation	Without Dark Energy perturbation
w_0	$-1.146^{+0.176+0.410}_{-0.178-0.305}$	$-1.118^{+0.152+0.324}_{-0.147-0.282}$
w_1	$0.600^{+0.622+0.802}_{-0.652-1.996}$	$0.499^{+0.453+0.675}_{-0.498-1.154}$
n_s	$0.962^{+0.016+0.033}_{-0.016-0.031}$	$0.955^{+0.014+0.027}_{-0.015-0.028}$
τ	$0.084^{+0.013+0.045}_{-0.012-0.046}$	$0.079^{+0.012+0.043}_{-0.012-0.046}$

identified with a constant effective equation of state[55]

$$w_{eff} \equiv \frac{\int da \Omega(a) w(a)}{\int da \Omega(a)}, \quad (10)$$

however the SNIa and LSS observations will break such a degeneracy with additional geometrical constraints. Thus for the realistic cases of including dark energy perturbations, the correlations between the dark energy and the background parameters as well as the auto correlations of the background cosmological parameters have been enlarged, as can be seen from Fig.3.

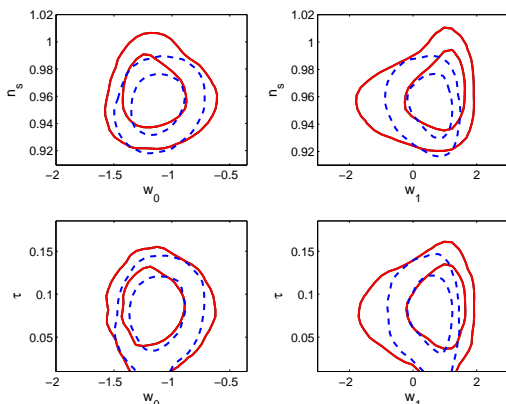


FIG. 4: Contour plot of w_0 and w_1 . Here we use the same parametrization and data sets as FIG.2, red solid and blue dashed lines are for perturbed and unperturbed DE respectively.

Dark energy perturbation affect dark energy parameters most directly and significantly, which can also be seen from Fig.4 on the constrains in the (w_0, w_1) plane. For the parameters (w_0, w_1) the inclusion of the dark energy perturbation change its best fit values from $(-1.212, 0.839)$ to $(-1.363, 1.325)$. Dark energy perturbation introduces more degeneracy between w_0 and w_1 thus enlarges the contours a lot. From the figure we can see that dynamical dark energy with the four types are all allowed by the current observations and Quintom A seems to cover the largest area in the 2-dimensional contours with all the data we used.

As shown in Fig.3 that w_0 and w_1 are in strong correlations. The constraints on $w(z)$ are perhaps relatively model independent, as suggested by Ref.[41].

Following[57] we obtain the constraints on $w(z)$ by computing the median and $1, 2\sigma$ intervals at all redshifts up to $z = 2$. In Fig.5 we plot the behavior of the dark energy EOS as a function of redshift z , we find that at redshift $z \sim 0.3$ the constraint on the EOS is relatively very stringent. One can see that the perturbation reinforces the trend of DE to cross -1 at $z \sim 0.3$. However despite in some sense $w(z)$ is well constrained by the current data, the quintom scenario is only favored at $\sim 1\sigma$ by the full dataset from CMB, LSS and SNIa. The accumulation of the observational data are still urged especially when for the probe of the dynamical dark energy. We find the value at $z = 0.3$ is restricted at

$$w(z = 0.3) = -1.003^{+0.100+0.229}_{-0.096-0.191} \quad (11)$$

for the case without dark energy perturbations and

$$w(z = 0.3) = -1.008^{+0.003+0.294}_{-0.115-0.299} \quad (12)$$

when including dark energy perturbations. Correspondingly at redshift $z = 1$ the constraints turn out to be

$$w(z = 1) = -0.869^{+0.149+0.230}_{-0.160-0.407} \quad (13)$$

without perturbations and

$$w(z = 1) = -0.846^{+0.209+0.277}_{-0.221-0.789} \quad (14)$$

when including dark energy perturbations. One should bear in mind that such a constraint is not really model independent, as shown in Refs. [58, 59].

Discussion and conclusion. In this paper we have performed a first analysis on dynamical dark energy from the latest WMAP three year as well as the SN Ia and LSS information. Our results show that when we include the perturbations of dark energy, the current observations allow for a large variation in the EOS of dark energy with respect to redshift. A dynamical dark energy with the EOS getting across -1 is favored at around 1σ with the combined constraints from the latest WMAP, SDSS and the "gold" dataset of SNIa by Riess *et al.*

Compared with our pre-WMAP-3 results[14] we find now the constraints on dark energy parameter space are improved significantly. This lies on the fact that the CMB observations have been improved significantly and

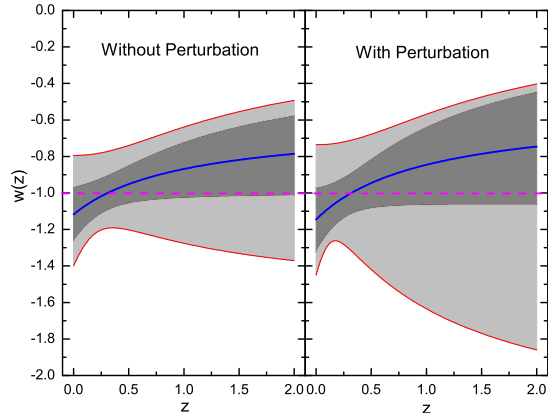


FIG. 5: Constrains on $w(z)$ using WMAP + 157 "gold" SNIa data + SDSS with/without DE perturbation. Median (central line), 68% (inner, dark grey) and 95% (outer, light grey) intervals of $w(z)$ using 2 parameter expansion of the EOS in (4).

also an inclusion of the smaller scale power of the Lyman α also help a lot to break the degeneracies. We also note in addition to the discrepancy between WMAP-3 and the Riess sample of "Gold" SNIa, WMAP-3 also prefers a lower value of σ_8 . σ_8 is an important quantity characterizing the size of fluctuations on the galactic scales and this will have some profound implications on the studies of structure formations. On the other hand Lyman α data prefers a higher value of σ_8 and in some sense, our current method of global fittings are not very strong in the probe of such discrepancies unless all the noteworthy inconsistencies are all due to neglecting the dynamics of dark energy. While the current WMAP-3 data and the WMAP + SDSS combination favor both a deviation from $n_S = 1$ and $w = -1$, where some nontrivial dynamics might be available "simultaneously" the both phases of accelerated expansions more parameters character-

ing the dynamics and inherent physical quantities like the tensor to scalar ratio r of the primordial spectrum, running of the scalar spectral index $dn_S/d\ln k$ and also the running of w as shown in the current paper need also to be considered for both probes of the dynamics and also to avoid some possible bias due to simply assuming no dynamics in one sector [50]. Moreover in our current study we have neglected the secondary Sunyaev-Zeldovich (SZ) effects in CMB calculations, which can also give rise to some minor shifts on the parameter space. But as indicated in Ref. [1] such shifts are typically small and the error bars on cosmological parameter estimations are similar when compared with cases neglecting the SZ effects. Further detailed analysis on the implications of dynamical dark energy in light of the current observations are currently in progress.

In our all results, the perturbation of dark energy plays a significant role in the determination of cosmological parameters. Neglecting the contributions of dark energy perturbation will lead to biased results as shown explicitly. In the next decade, many ongoing projects in the precise determination of cosmological parameters will be available. We can hopefully detect the signatures of dynamical dark energy like quintom through global fittings to the observations, where it is crucial for us to include the contributions of dark energy perturbations.

Acknowledgements: We acknowledge the use of the Legacy Archive for Microwave Background Data Analysis (LAMBDA). Support for LAMBDA is provided by the NASA Office of Space Science. Our MCMC chains were finished in the Shuguang 4000A system of the Shanghai Supercomputer Center (SSC). This work is supported in part by National Natural Science Foundation of China under Grant Nos. 90303004, 10533010 and 19925523 and by Ministry of Science and Technology of China under Grant No. NKBRSF G19990754. We are indebted to Patrick McDonald for clarifying correspondence on the fittings to the Lyman α data. We thank Sarah Bridle, Antony Lewis, Mingzhe Li, Hong Li Jun'ichi Yokoyama and PengJie Zhang for helpful discussions and comments on the manuscript.

[1] D. N. Spergel *et al.*, arXiv:astro-ph/0603449.
[2] L. Page *et al.*, arXiv:astro-ph/0603450. G. Hinshaw *et al.*, arXiv:astro-ph/0603451. N. Jarosik *et al.*, arXiv:astro-ph/0603452.
[3] M. Tegmark *et al.* (SDSS Collaboration), *Astrophys. J.* **606**, 702 (2004).
[4] S. Weinberg, *Rev. Mod. Phys.* **61**, 1 (1989).
[5] I. Zlatev, L.-M. Wang, and P. J. Steinhardt, *Phys. Rev. Lett.* **82**, 896 (1999).
[6] R. D. Peccei, J. Sola and C. Wetterich, *Phys. Lett. B* **195**, 183 (1987); C. Wetterich, *Nucl. Phys. B* **302**, 668 (1988); C. Wetterich, *Astron. Astrophys.* **301**, 321 (1995).
[7] B. Ratra and P. J. E. Peebles, *Phys. Rev. D* **37**, 3406 (1988); P. J. E. Peebles and B. Ratra, *Astrophys. J.* **325**,

L17 (1988).
[8] A.G. Riess *et al.* (Supernova Search Team Collaboration), *Astron. J.* **116**, 1009 (1998).
[9] S. Perlmutter *et al.* (Supernova Cosmology Project Collaboration), *Astrophys. J.* **517**, 565 (1999).
[10] J. L. Tonry *et al.* (Supernova Search Team Collaboration), *Astrophys. J.* **594**, 1 (2003).
[11] A. G. Riess *et al.* (Supernova Search Team Collaboration), *Astrophys. J.* **607**, 665 (2004).
[12] A. Clocchiatti *et al.* (the High Z SN Search Collaboration), arXiv:astro-ph/0510155.
[13] P. Astier *et al.*, arXiv:astro-ph/0510447.
[14] J. Q. Xia, G. B. Zhao, B. Feng, H. Li and X. Zhang, arXiv:astro-ph/0511625.

- [15] R. R. Caldwell, Phys. Lett. B **545**, 23 (2002).
- [16] S. M. Carroll, M. Hoffman and M. Trodden, Phys. Rev. D **68**, 023509 (2003); J. M. Cline, S.-Y. Jeon and G. D. Moore, Phys. Rev. D **70**, 043543 (2004).
- [17] e. g. P. H. Frampton, Phys. Lett. B **555**, 139 (2003); V. Sahni and Y. Shtanov, J. Cosmol. Astropart. Phys. **0311**, 014 (2003); B. McInnes, J. High Energy Phys. **0208**, 029 (2002); V.K. Onemli and R.P. Woodard, Class. Quant. Grav. **19**, 4607 (2002); V. K. Onemli and R. P. Woodard, Phys. Rev. D **70**, 107301 (2004); I. Y. Aref'eva, A.S. Koshelev and S.Y. Vernov, astro-ph/0412619; I. Y. Aref'eva and L. V. Joukovskaya, JHEP **0510**, 087 (2005).
- [18] S. Nesseris and L. Perivolaropoulos, Phys. Rev. D **70**, 043531 (2004).
- [19] U. Alam, V. Sahni and A. A. Starobinsky, J. Cosmol. Astropart. Phys. **0406**, 008 (2004).
- [20] D. Huterer and A. Cooray, Phys. Rev. D **71**, 023506 (2005).
- [21] B. Feng, X. Wang, and X. Zhang, Phys. Lett. B **607**, 35, (2005).
- [22] e.g. J. Weller and A. Albrecht, Phys. Rev. Lett. **86**, 1939 (2001); Y. Wang and P. Mukherjee, Astrophys. J. **606**, 654 (2004); Y. Wang and M. Tegmark, Phys. Rev. Lett. **92** (2004) 241302; U. Alam, V. Sahni, T. D. Saini, and A. A. Starobinsky, Mon. Not. Roy. Astron. Soc. **354**, 275 (2004); Z. H. Zhu, M. K. Fujimoto, and X. T. He, Astron. Astrophys. **417**, 833 (2004); Y. Gong, Class. Quant. Grav. **22**, 2121 (2005); Z.-H. Zhu, Astrophys. J. **620**, 7 (2005); G. Chen and B. Ratra, Astrophys. J. **612**, L1 (2004); Y. Wang, J. M. Kratochvil, A. Linde and M. Shmakova, J. Cosmol. Astropart. Phys. **0412**, 006 (2004); W. Godlowski and M. Szydlowski, Gen. Rel. Grav. **36**, 767 (2004); D. Rapetti, S. W. Allen and J. Weller, Mon. Not. Roy. Astron. Soc. **360**, 555 (2005); J. Simon, L. Verde and R. Jimenez, Phys. Rev. D **71**, 123001 (2005); C. Csaki, N. Kaloper and J. Terning, Annals Phys **317**, 410 (2005); E. Majerotto, D. Sapone and L. Amendola, astro-ph/0410543; M. P. Dabrowski and T. Stachowiak, hep-th/0411199; L. Perivolaropoulos, Phys. Rev. D **71**, 063503 (2005); Z.-H. Zhu, Astrophys. J. **620**, 7 (2005); Y. Gong and Y.-Z. Zhang, astro-ph/0502262; S. Hannestad, Phys. Rev. D **71**, 103519 (2005); G. Olivares, F. Atrio-Barandela and D. Pavon, Phys. Rev. D **71**, 063523 (2005); W. Wang, Y.-X. Gui, S.-H. Zhang, G.-H. Guo and Y. Shao, astro-ph/0504094; M. Szydlowski, W. Godlowski, A. Krawiec and J. Golbiak, astro-ph/0504464; L. Perivolaropoulos, astro-ph/0504582; X. Zhang and F.-Q. Wu, astro-ph/0506310; B. Wang, Y. Gong and E. Abdalla, hep-th/0506069; M.-X. Luo and Q.-P. Su, astro-ph/0506093; Z.-H. Zhu and J.S. Alcaniz, Astrophys. J. **620**, 7 (2005); C. Csaki, N. Kaloper and J. Terning, astro-ph/0507148; M. Ishak, A. Upadhye and D. N. Spergel, astro-ph/0507184; D. Polarski and A. Ranquet, astro-ph/0507290; J. S. Alcaniz and J. A. S. Lima, astro-ph/0507372; S. Nesseris and L. Perivolaropoulos, astro-ph/0511040.
- [23] T. Chiba, T. Okabe and M. Yamaguchi, Phys. Rev. D **62** (2000) 023511.
- [24] C. Armendariz-Picon, V. Mukhanov and P. J. Steinhardt, Phys. Rev. Lett. **85**, 4438 (2000); Phys. Rev. D **63**, 103510 (2001).
- [25] A. Vikman, Phys. Rev. D **71**, 023515 (2005).
- [26] G. B. Zhao, J. Q. Xia, M. Li, B. Feng and X. Zhang, Phys. Rev. D **72**, 123515 (2005).
- [27] L. R. Abramo and N. Pinto-Neto, astro-ph/0511562.
- [28] B. Feng, M. Li, Y. S. Piao and X. Zhang, astro-ph/0407432.
- [29] Z.-K. Guo, Y.-S. Piao, X. Zhang and Y.-Z. Zhang, Lett. B **608**, 177, (2005).
- [30] W. Hu, Phys. Rev. D **71** (2005) 047301.
- [31] X. Zhang, hep-ph/0410292.
- [32] R. R. Caldwell and M. Doran, Phys. Rev. D **72**, 043527 (2005).
- [33] X.-F. Zhang, H. Li, Y.-S. Piao, and X. Zhang, astro-ph/0501652.
- [34] For an interesting variation see H. Wei, R. G. Cai and D. F. Zeng, Class. Quant. Grav. **22**, 3189 (2005) and for another single-field quintom model see e.g. C. G. Huang and H. Y. Guo, astro-ph/0508171.
- [35] I. Brevik, O. Gorbunova, gr-qc/0504001; I. Ya. Aref'eva, A.S. Koshelev, S.Yu. Vernov, astro-ph/0507067; G.V. Vereshchagin, astro-ph/0511131; B.M.N. Carter and I.P. Neupane, hep-th/0510109; H. Stefancic, Phys. Rev. D **71** (2005) 124036; Z. Chang, F. Q. Wu and X. Zhang, Phys. Lett. B **633**, 14 (2006); J. Alcaniz and H. Stefancic, arXiv:astro-ph/0512622; and references therein.
- [36] M. Li, B. Feng and X. Zhang, hep-ph/0503268.
- [37] S. W. Hawking and T. Hertog, Phys. Rev. D **65**, 103515 (2002).
- [38] Ch. Yeche, A. Ealet, A. Refregier, C. Tao, A. Tilquin, J.-M. Virey and D. Yvon, astro-ph/0507170.
- [39] P. S. Corasaniti, M. Kunz, D. Parkinson, E. J. Copeland and B. A. Bassett, Phys. Rev. D **70**, 083006 (2004).
- [40] S. Hannestad and E. Mortsell, J. Cosmol. Astropart. Phys. **0409** 001 (2004); A. Upadhye, M. Ishak and P. J. Steinhardt, Phys. Rev. D **72**, 063501 (2005).
- [41] U. Seljak *et al.*, Phys. Rev. D **71**, 103515 (2005).
- [42] J. Weller and A. M. Lewis, Mon. Not. Roy. Astron. Soc. **346**, 987 (2003).
- [43] For a relevant study see e.g. R. Bean and O. Dore, Phys. Rev. D **69**, 083503 (2004).
- [44] P. McDonald *et al.*, arXiv:astro-ph/0407377.
- [45] D. Gamerman, *Markov Chain Monte Carlo: Stochastic simulation for Bayesian inference* (Chapman and Hall, 1997).
- [46] D. J. C. MacKay (2002), <http://www.inference.phy.cam.ac.uk/mackay/itprnn/book.html>.
- [47] R. M. Neil (1993), <ftp://ftp.cs.utoronto.ca/pub/~radford/review>.
- [48] M. Chevallier and D. Polarski, Int. J. Mod. Phys. D **10**, 213(2001); E. V. Linder, Phys. Rev. Lett. **90**, 091301 (2003).
- [49] C. -P. Ma and E. Berschinger, Astrophys. J. **455** 7, (1995).
- [50] J. Q. Xia, G. B. Zhao, B. Feng and X. Zhang, arXiv:astro-ph/0603393.
- [51] A. Lewis and S. Bridle, Phys. Rev. D **66**, 103511 (2002).
- [52] W. L. Freedman *et al.*, Astrophys. J. **553**, 47 (2001).
- [53] S. Burles, K. M. Nollett and M. S. Turner, Astrophys. J. **552**, L1 (2001).
- [54] M. Tegmark *et al.* (SDSS Collaboration), Phys. Rev. D **69**, 103501 (2004).
- [55] e.g. L. M. Wang, R. R. Caldwell, J. P. Ostriker and P. J. Steinhardt, Astrophys. J. **530**, 17 (2000).
- [56] See e.g. G. N. Felder, A. V. Frolov, L. Kofman and A. V. Linde, Phys. Rev. D **66** (2002) 023507.
- [57] D. Huterer and M. S. Turner, Phys. Rev. D **64**, 123527 (2001).

- [58] B. A. Bassett, P. S. Corasaniti and M. Kunz, *Astrophys. J.* **617**, L1 (2004). **20**, 2409 (2005).
- [59] J.-Q. Xia, B. Feng, and X. Zhang, *Mod. Phys. Lett. A*